

Research article

Projecting China's future water footprint under the shared socio-economic pathways



Xiaocong Xu¹, Yuanying Zhang¹, Yimin Chen^{*}

Guangdong Provincial Key Laboratory of Urbanization and Geo-simulation, School of Geography and Planning, Sun Yat-sen University, Guangzhou, 510275, PR China

ARTICLE INFO

Keywords:

Water footprint

MRIO model

Land use simulation

Shared socio-economic pathways

ABSTRACT

Increasing water scarcity in China is further exacerbated by the rapid socio-economic development and uneven spatial distribution of water resources. Current studies on water footprint have mainly focused on historical accounting and trend analysis at the provincial scale. However, a comprehensive exploration of future water footprint would be vital to a better understanding of future water shortage challenges, and more importantly, would allow the mitigation of water scarcity and unequal water distribution. In this paper, we present an approach to project the future water footprint of China at a fine resolution (0.125 arc-degree) under the shared socio-economic pathway (SSP) scenario framework, which described five future alternative socio-economic development pathways over the 21st century. We first simulated the future spatial patterns of built-up land using the Future Land Use Simulation (FLUS) model and derived the future population growth and urbanization rate from the population projection provided by the National Center for Atmospheric Research (NCAR). Then future water footprint was projected according a log-transformed linear regression calibrated with historical data during 2007–2012. We found that the total volume of China's water footprint will increase significantly in the future under the SSP1, SSP4 and SSP5 scenarios, reaching up to nearly 400 billion m³ in 2050, equivalent to almost 40% increase compared to that in 2010. The spatial patterns of future water footprint show dramatic increase (up to 100–130%) in the eastern provinces (Shandong, Henan, and Hebei), and slight decrease were found in the western provinces (Xinjiang, Ningxia, and Qinghai). In addition, the future water footprints were found to share very similar spatial patterns at local pixel scale among different SSP scenarios in three of the largest metropolitan areas of China (Beijing-Hebei-Tianjin, Yangtze River Delta, and Pearl River Delta). These findings provide extensive knowledge of the future water footprint and suggest a more severe water scarcity in the future from a consumption-oriented perspective. More effective water management policies are urgently needed to mitigate future water resource scarcity and inequality.

1. Introduction

Increasing pressure on Earth's freshwater resources owing to increasing human demands has become a threat to sustainable development and has drawn considerable attention at local and global scales (Mekonnen and Hoekstra, 2016). Jointly driven by population growth and socio-economic development, the global water use has been increasing by approximately 1% annually since the 1980s (WWAP, 2019). This trend is expected to last until 2050 and results in an increase of 20–30% in water usage (Burek et al., 2016). As a rapidly developing country, China is facing severe water scarcity issues due to widespread urbanization process and population growth (Liu and Yang, 2012). This

challenge is further intensified by the uneven distribution of water resources leading to a spatial mismatch between demand and availability of water. In particular, drier provinces in northern China produce water-intensive goods and export them to water-rich coastal provinces in east and south China (Feng et al., 2014). This situation was getting worse over the past few decades (Jiang, 2009; Liu and Yang, 2012). In response to the regional water scarcity, the Government of China has implemented numerous physical water transfer projects, among which the South-North Water Transfer Project is the largest (Liu et al., 2013). Although water scarcity issues in northern China might be partially mitigated through water imports, a series of negative ecological consequences are predicted to be introduced in southern China (Lin et al.,

* Corresponding author.

E-mail address: chenym49@mail.sysu.edu.cn (Y. Chen).

¹ Co-first authors and contributed equally to the article.

2012).

Another perspective towards mitigating regional water scarcity is to incorporate the concepts of virtual water and water footprint, which have drawn increasing attentions in recent years (Vörösmarty et al., 2015). Originally, virtual water was proposed by Allan (1998) to illustrate the total quantity of water resources embodied within water-intensive goods along the entire production chain. In this case, the water resources are virtually transferred through trade between regions, typically referred as virtual water flows (Dietzenbacher and Velazquez, 2007). "Water footprint", analogous to "ecological footprint", is a consumption-oriented indicator that represents the total quantity of virtual water consumed by individuals and administrative units (Hoekstra and Hung, 2003). It focuses on the virtual water use beyond the scales of region and sector (Feng et al., 2017; Oki and Kanae, 2004). According to previous research (Hoekstra and Mekonnen, 2012), the annual water footprint per capita of China is slightly below the global average (1385 m³ per year per capita). However, China was the largest water footprint consumption country in the world during 1996–2005 consuming a total amount of 1368 Gm³ fresh water annually over this period, mainly attributed to its massive population of 1.3 billion people (approximately 1/5th of the world population).

A number of studies have been conducted to evaluate and investigate water footprint consumption at regional and global scales. The methods used in majority of these studies for accounting water footprint fall into two categories: production tree method and input-output model. The production tree method has been more commonly applied to account for the water footprint of agricultural and animal products, including crop (Hoekstra and Hung, 2003), cotton (Chapagain et al., 2006), potato (Rodriguez et al., 2015), and poultry and livestock (Gerbens-Leenes et al., 2013). The input-output model, especially the multi-region input-output (MRIO) model, is a more popular approach to calculate virtual water flow and water footprint for various sectors in different regions with the aid of input-output tables and water use data. For example, Lenzen et al. (2013) quantified the global virtual water trade for the year 2000 using the global MRIO dataset. An extensive review on the application of input-output model for the investigation of large-scale environmental impacts, such as greenhouse gas emissions, carbon and water footprint, can be found in Hawkins et al. (2015).

The spatial patterns of water footprint in China for some specific provinces/basins have been reported during the past decade. For example, Zhang et al. (2011) estimated the water footprint of Beijing in 2002 using a 30-region 33-sector MRIO analysis. Zhang and Anadon (2014) quantified the structure of trade-based virtual water flow among the provinces in China in 2007 based on a MRIO model and estimated the water footprint of each province. They found that the more developed coastal provinces have a much greater volume of water footprint per capita than those located in the inland and western provinces. Deng et al. (2016) calculated the regional water footprint of China in 2002 and 2007 and analyzed its trend. They concluded that the water footprint pattern in each region of China has changed significantly from 2002 to 2007, and up to 70% of water was consumed by the agricultural sector. Although there are number of studies on water footprint estimation and driver analysis, majority of them focused on historical accounting and analysis based on the input-output analysis in single or multiple years for which the input-output tables are available. To the best of our knowledge, no studies have been conducted on the projection of water footprint patterns in the future scenarios; a comprehensive exploration of water footprint in the foreseeable future is significant for better understanding of future water shortage challenges and for implementing the mitigation measures for the pressing issues of water scarcity and inequality. Moreover, with a few exceptions (Hoekstra and Mekonnen, 2012), existing studies usually conducted their accounting at regional levels (provinces, basins, and nations); the spatial heterogeneity within the administrative units were not fully taken into consideration.

This study aims at the projection of future water footprint pattern of China at a fine spatial resolution (0.125 arc-degree). The water footprint

consumption is driven by a series of socio-economic factors, among which the urbanization associated with urban expansion and population growth is an essential factor. Thus, the future water footprint projection involves the future simulation of land use patterns. In the past two decades, a series of land use and cover change simulation models based on the cellular automata (CA) have been developed to simulate the land use dynamics (Clarke and Gaydos, 1998; Dietzel and Clarke, 2007; Li and Yeh, 2002; Verburg et al., 2002). Extensive efforts have been made to improve model performance including transition rules calibrations (Chen et al., 2016; He et al., 2013; Rienow and Goetzke, 2015), neighborhood configurations (Kocabas and Dragicevic, 2006; Yeh and Li, 2006), and high-performance optimization for large scale applications (Guan et al., 2016; Li et al., 2010). Most up-to-date CA-based models have been proven to be effective and reliable for urban expansions and even multi-type land use changes under different scenarios (Li et al., 2017; Liu et al., 2017). Future water footprint consumption associated with future socioeconomic development depends greatly on development strategies. We carried out the future land use simulation and the water footprint projection under the shared socio-economic pathway (SSP) scenarios developed by the intergovernmental panel on climate change (IPCC) (O'Neill et al., 2017). The SSP scenario framework provides five future alternative socio-economic development pathways over the 21st century with narratives combining different challenges for mitigation and adaptation (Riahi et al., 2017). Thus, it can comprehensively reflect the complexity of future urban expansion and population growth, and the projected water footprint results are comparable among the different geographic regions and cross-disciplines as they share the same scenario assumptions (Zhang et al., 2017).

In this study, we followed four steps to project the future water footprint patterns in China under the SSP scenario framework: 1) We estimated the provincial water footprint in 2007, 2010, and 2012 via a 30-region 30-sector MRIO analysis; 2) Multi-linear regression was used to investigate the associated drivers of water footprint consumption such as population, gross domestic product (GDP) per capita, urbanization rate, construction land, etc.; 3) Spatial pattern of drivers that pass the significant test in step 2 were projected under the SSP scenario framework; 4) The future water footprint patterns were projected using the regression analysis. In step 3, the future pattern of the built-up land was simulated using the CA-based Future Land Use Simulation (FLUS) model (Liu et al., 2017). In step 4, the spatial heterogeneity of water footprint was achieved by assuming that the drivers are similar between the provinces and the 0.125 arc-degree pixel scale, analogous to previous studies of mapping fine scale population distribution (Jia et al., 2014) and carbon emissions (Meng et al., 2017). In addition, the final projected water footprints were adjusted by applying a provincial constraint. More details are provided in the Methodology section.

2. Dataset

2.1. Input-output tables and water use data

Data for estimating the provincial water footprints include the Inter-regional Input-Output Tables of China in years of 2007 (Liu et al., 2012), 2010 (Liu et al., 2014) and 2012 (Mi et al., 2017). These tables provide the transactional monetary flows among the different provinces and sectors. A total of 30 provincial units are included in these tables, including 22 provinces, 4 municipalities and 4 autonomous regions (regions of Tibet province, Hongkong, Macao and Taiwan are not included). We refer them consistently as provinces throughout this paper for simplicity. For each province, the data are divided into 30 economic sectors, with one aggregated agricultural sector and other 29 non-agricultural sectors. Water consumption data for each province by sector were obtained from the water resource bulletins (<http://www.mwr.gov.cn/english/pubs/>), the Bulletin of First National Census for Water (Ministry of Water Resources, 2013) and other statistical data from the National Bureau of Statistics of China (<http://www.stats.gov>.

cn/english/). These data were used to estimate the direct water use coefficients for different provinces and sectors, which are fundamental to water footprint accounting.

2.2. Land use data

The historical built-up land data were extracted from the land use maps of China for the years 2008, 2010, and 2013, developed by the Chinese Academy of Sciences (CAS). These land use maps had a spatial resolution of $1 \times 1 \text{ km}^2$. Built-up land areas were extracted from these maps by aggregating the sub-categories of rural residential land, urban residential land and industrial land. The digital elevation model (DEM) data and the spatial distributions of cities, counties, high-speed railway stations, and rivers were collected and used to generate distance variables that represent the driving factors of land use change (see Supplementary Fig. S1). The DEM data is provided by the National Aeronautics and Space Administration (NASA) Shuttle Radar Topographic Mission (SRTM) with a resolution of $90 \times 90 \text{ m}$. The driving variables were generated and processed with the ArcMap software developed by the ESRI company. To keep consistent with the spatial resolution of land use maps, we resampled the SRTM DEM data into $1 \times 1 \text{ km}^2$ resolution using the Resample tool with the bi-linear interpolation technique. The slope map was generated using the Slop tool based on the original $90 \times 90 \text{ m}^2$ resolution SRTM DEM data and then was resampled into $1 \times 1 \text{ km}^2$. The patterns of distance variables (e.g., distances to city center, railway, etc.) were generated using the Euclidean Distance tool at $1 \times 1 \text{ km}^2$ resolution. Since the data of input-output tables do not include regions of Tibet province, Hongkong, Macao, and Taiwan, these four regions were excluded in the built-up land simulations and water footprint projections.

2.3. Socio-economic data

Historical statistics of population and GDP in each of the provinces in 2000, 2007, 2010, and 2012 were collected from the China Population Statistics Yearbooks (<http://www.stats.gov.cn/english/StatisticalData/AnnualData/>) assembled by the National Bureau of Statistics of China. Future projections of population were obtained from the Climate and Global Dynamics Laboratory of the National Center for Atmospheric Research (NCAR) (Jones and O'Neill, 2016), which is hereinafter referred to as NCAR population projection. It provides a spatially explicit estimation of population under five SSPs scenarios for the next hundred year, with a spatial resolution of 0.125 arc-degree. They were used to project the future amounts of built-up land demand and water footprint under different SSPs scenarios. Since projections in the starting year (2000) varied slightly from the population statistics within the China region, we applied a linear scaling to adjust these population projections (see details in Methodology section).

3. Methodology

3.1. Water footprint accounting

The provincial water footprint is accounted based on MRIO analysis. Suppose that there are m provinces and each province is divided into n economic sectors. The total outputs for each province is equal to the sum of the total intermediate inputs and the final consumption, which can be expressed using a balanced equation as follows (Miller and Blair, 2009; Zhang and Anadon, 2014):

$$x_i^R = \sum_{S=1}^m \sum_{j=1}^n x_{ij}^{RS} + \sum_{S=1}^m y_i^{RS} \quad (1)$$

where x_i^R represent province R 's total outputs; x_{ij}^{RS} is the intermediate inputs from sector i in province R to sector j in province S ; and y_i^{RS} is the final consumption of sector i in province S supplied by province R . By

applying a direct input coefficient a_{ij}^{RS} , Equation (1) can be transformed into:

$$x_i^R = \sum_{S=1}^m \sum_{j=1}^n a_{ij}^{RS} x_j^S + \sum_{S=1}^m y_i^{RS} \quad (2)$$

$$a_{ij}^{RS} = x_{ij}^{RS} / x_j^S \quad (3)$$

where a_{ij}^{RS} is the direct input coefficient, representing the total amount of products required from sector i in province R to produce one unit of product in sector j in province S . As to a system with multiple interdependent regions and sectors, Equation (2) can be expressed as a matrix form as follows:

$$X^* = A^* X^* + Y^* \quad (4)$$

where $X^* = [x_i^R]$ denotes the output matrix; $A^* = [a_{ij}^{RS}]$ denotes the direct consumption matrix; and $Y^* = y_i^{RS}$ denotes the final demand matrix. By introducing the inversed Leontief matrix $B^* = (I - A^*)^{-1}$, Equation (4) can be transformed into:

$$X^* = (I - A^*)^{-1} Y^* \quad (5)$$

where I is an identity matrix with the same order as A^* . The element b_{ij}^{RS} in the inversed Leontief matrix represents the outputs of sector i in province R required to satisfy one monetary unit of final consumption of sector j in province S . Based on Equation (5), it is feasible to estimate the change of output of a sector affected by the change of the final demand. Analogue to previous studies, we introduce a direct water use coefficient matrix W^* , whose element represents the water consumption to produce one unite of product of sector i in province R :

$$W^* = [w_i^R / x_i^R] \quad (6)$$

Then the water footprint among different provinces with multiple sectors can be estimated by multiplying the direct water use coefficient matrix by the output matrix, as follows:

$$\begin{aligned} F^* &= W^* X^* \\ &= W^* (I - A^*)^{-1} Y^* \end{aligned} \quad (7)$$

where F^* represents the water footprint of different sectors in different provinces. In some previous studies (Han et al., 2018; Zhang et al., 2018), the term $W^* (I - A^*)^{-1}$ is defined as the total water consumption coefficient matrix Q^* :

$$Q^* = W^* (I - A^*)^{-1} \quad (8)$$

Thus, the water footprint matrix F^* can also be expressed as the multiplication of the total water consumption coefficient matrix Q^* by the final demand matrix Y^* :

$$\begin{aligned} F^* &= W^* (I - A^*)^{-1} Y^* \\ &= Q^* \times Y^* \end{aligned} \quad (9)$$

3.2. Built-up land change simulation

The dynamic patterns of future built-up land were simulated using an integrated model consisting of two interactively coupling components. One is the top-down approach to project the future macro land use demand, and the other one is a bottom-up model to simulate the local land patch evolutions. In this study, the future built-up land demand of each province under different SSP scenarios were projected with a MRIO analysis, following the methodology proposed by Chen et al. (2019). Thereafter, we used a CA-based approach, namely the Future Land Use Simulation FLUS model (Liu et al., 2017), to simulate the local land use evolution at a spatial resolution of $1 \times 1 \text{ km}^2$ under the given built-up land demand.

In the FLUS model, the land use pattern evolves through the study

period. Specifically, as to a non-built-up land patch, it either retains the current state or transforms into built-up land according to the transformation probability and the roulette selection mechanism. In this study, the transformation probability was estimated according to the suitability S , the neighborhood effect Ω , the inertia factor $Inertia$, and the conversion cost sc , as follows (Liu et al., 2017):

$$TP_p^t = S_p \times \Omega_p^t \times Inertia^t \times (1 - sc_k) \quad (10)$$

where TP_p^t is the transformation probability of a land patch p to transform from non-built-up to built-up land at iteration time t ; S_p is the suitability for the land patch on location p to develop into built-up land; Ω_p^t is the neighborhood effect of land patch p at time t , denoting developing influence from the surrounding patches; $Inertia^t$ is the inertia factor that controls the conversion pace of the evolution; sc_k is the conversion cost of land use type k converted to built-up land.

The suitability S_p for each land patch was assumed to be determined by the biophysical factors and socio-economical drivers (Sohl and Sayler, 2008), such as terrain, population, proximity to city site and road network. Many previous studies have adopted statistical and machine learning approaches to calibrate the suitability surface based on the given factors and drivers (Li and Yeh, 2000; Liu et al., 2008; Van Asselen and Verburg, 2013). We use the well-accepted machine learning approach, the artificial neural network (ANN), to establish the complex mapping between drivers and suitability, considering the effective nonlinear functionality of ANN (Li and Yeh, 2002). The ANN consists of one input layer, one output layer and twelve hidden layers. Neurons of the input layer correspond to the topographic factors and socio-economic drivers (see Supplementary Fig. S1); neurons in the output layer are the derived probability of built-up and non-built-up land. The back-propagation learning strategy (BP-ANN) was used to calibrate the weight matrix that connects the neurons between the adjacent layers. We used the Log-sigmoid function as the activation function to ensure that the output of the BP-ANN is within the range of 0–1. The mean square error (MSE) was used as the cost function to evaluate the performance of each training epoch in the training phase. To avoid overfitting problem, we stopped the training process in situations where either the MSE was below 0.001 or the MSE did not decrease during 10 epochs. Note that the suitability S_p estimated from the BP-ANN represents the fitness of a land patch to develop into built-up land at given spatial variables. Analogous to previous LUCC simulation approaches (Letourneau et al., 2012; Van Asselen and Verburg, 2013; Verburg et al., 2002), this suitability was assumed to remain unchanged during the entire study period.

The neighborhood effect accounts of the spatial autocorrelation of adjacent land patches. Similar to previous studies, the neighborhood was denoted as the built-up land density in the Moore neighborhood (Batty, 1997). Specifically, at a land patch p , the neighborhood effect at iteration time t can could be expressed as (Li et al., 2017):

$$\Omega_p^t = \frac{\sum_{N \times N} con(s^t = \text{build_up})}{N \times N - 1} \quad (11)$$

In the equation, the term $\sum_{N \times N} con(s^t = \text{build_up})$ denotes the number of land patches that have been converted into built-up land within the $N \times N$ size Moor neighborhood at iteration time t . Higher neighborhood effect will encourage the non-built-up land patch to develop into a built-up land.

The inertia factor in Equation (10) is an essential component in the land use evolution process, which represents the competition and interaction among different land use types by adjusting the inheritance of previous land use status. It is defined as (Li et al., 2017; Liu et al., 2017):

$$Inertia^t = \begin{cases} inertia^{t-1} & \text{if } |D^{t-1}| \leq |D^{t-2}| \\ inertia^{t-1} \times \frac{D^{t-2}}{D^{t-1}} & \text{if } D^{t-1} < D^{t-2} < 0 \\ inertia^{t-1} \times \frac{D^{t-1}}{D^{t-2}} & \text{if } D^{t-1} > D^{t-2} > 0 \end{cases} \quad (12)$$

In Equation (12), the D^{t-1} denotes the difference between the macro demand of built-up land and the allocated area of built-up land patch till iteration time $t-1$. The core idea of the inertia factor is that, if the evolution trend of the built-up land is consistent with the macro demand, i.e., $|D^{t-1}| \leq |D^{t-2}|$, then the inertia coefficient will remain as the previous value; otherwise, the inertia coefficient will dynamically increase itself to amend the evolution trajectory in the next iteration (Liu et al., 2017).

The conversion cost in the transformation probability represents the difficulty of a non-built-up land patch to develop into built-up land (Aerts and Heuvelink, 2002; Verburg et al., 2002). It reflects the intrinsic attributes of land uses without considering extrinsic influences such as technology development and climate change. The conversion costs of different land use type varies and is determined based on the expert knowledge using the analytic hierarchy process (Saaty, 1990). The conversion costs for different non-built-up land use types were presented in Supplementary Table S1.

After the transformation probability of each land patch has been estimated at every iteration time using Equation (10), the FLUS model determines whether a specific land patch transforms into built-up land or not according to the estimated transformation probability TP_p^t . Usually land patches with high TP_p^t values are more likely to transform into built-up land. However, land use evolution involves various stochastic processes and uncertain complexities, and should be addressed in the simulation. In the FLUS model, whether a land use patch will transform or not was determined using the roulette selection mechanism. The estimated transformation probabilities were used to construct the roulette wheel. A random number ranging from 0 to 1 was generated and compared with the constructed roulette wheel. The land patch was considered to transform into built-up land if this random number fell into built-up land sectors of the roulette. Through this roulette selection mechanism, land patches with lower transformation probability still have small chance to develop, which enables the model to simulate real-world leapfrog growth situation (Chen et al., 2016). For a more detailed description of the roulette selection mechanism, please refer to the study by Liu et al. (2017).

Prior to its application for future built-up land simulation, the FLUS model was evaluated by simulating the historical built-up land evolution from 2008 to 2013 and then compared it with the actual land use pattern in 2013. The stratified sampling technique was used to generate the dataset for calibration and validation. A total number of 184,000 samples (2% of the total grid of both developed and undeveloped types) were randomly selected from the study region, of which 75% were used to calibrate the FLUS model and the rest 25% were used for validation. During the historical simulation, the gain area of built-up land was set as equal to the observed newly developed built-up land from 2008 to 2013.

To quantitatively evaluate the simulation, we adopted the indicator of 'Figure of Merit' (FoM) to evaluate the performance of simulation (Pontius et al., 2008, 2011). It is calculated as the ratio of correctly predicted change to the union of observed and predicted changes (Pontius et al., 2008):

$$FoM = \frac{B}{A + B + C + D} \quad (13)$$

where B denotes the area correctly predicted as changed; A denotes the observed changed area that is predicted as unchanged; C denote the observed changed area that is predicted as changed into the wrong category; D denotes the unchanged area that is predicted as changed. According to this equation, the FoM indicator focuses on the change

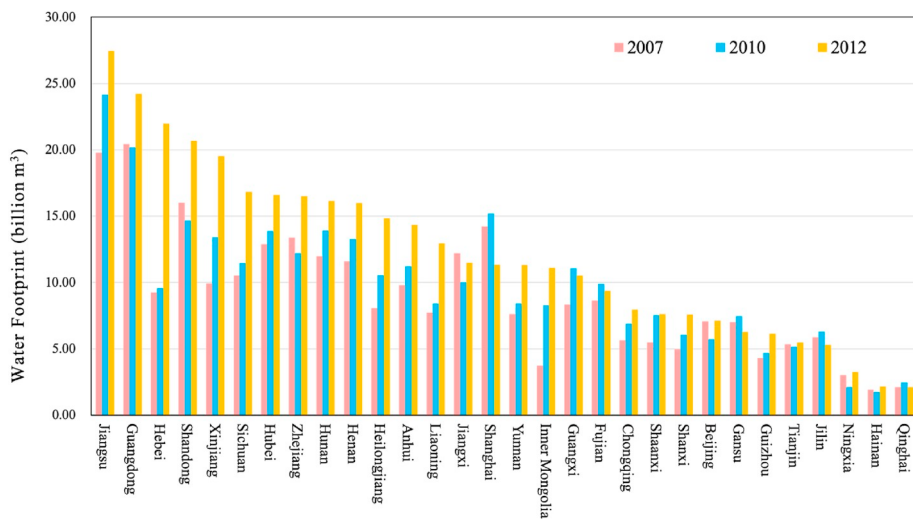


Fig. 1. Provincial water footprint and its trends in 2007, 2010, and 2012.

prediction rather than the overall pattern agreement, thus avoiding biases introduced by the persistent non-changed areas in traditional assessment metrics, such as overall accuracy and Kappa coefficient.

3.3. Estimation of future water footprint

The future water footprints under different SSP scenarios were projected based on the extrapolation of historical conditions of socio-economic variables. According to previous studies, variables of population, urbanization rate, GDP per capita, built-up land area, and agriculture land area were considered. A log-transformed linear regression was used to study the drivers of water footprint at the provincial scale using historical data acquired in 2007, 2010, and 2012:

$$\log_{10}(W\hat{F}) = \sum w_i \times \log_{10}(\text{var}_i) + \text{const} \quad (14)$$

where $W\hat{F}$ is the fitted water footprint; var_i is the independent variable weighted by the w_i ; and const is the constant term of the regression. A log transformation $\log_{10}(\cdot)$ was adopted to eliminate the collinearity and heteroscedasticity among the independent variables. A t -test was used to determine whether these five independent variables were significant in the regression analysis with a significance level of $\alpha = 0.05$. A total of 90 samples (30 provinces per year) in 2007, 2010, and 2012 were used to calibrate the weight coefficients w_i in Equation (14). The provincial water footprints were accounted according to the MRIO analysis (see Section 3.1). The population and GDP per capita were acquired from China Statistics Yearbook. The urbanization rate was derived based on the ratio between urban and rural populations from the China Statistics Yearbook. The built-up land and agriculture land areas were counted based on land use dataset developed by the CAS. We tested multiple combinations of independent variables, and chose the one in which all independent variables pass the significance test with a significance level of $\alpha = 0.05$.

The calibrated linear regression was used to project future water footprint pattern under five SSP scenarios. In order to obtain spatial heterogeneity within the administrative boundaries, an assumption was made that the calibrated regression at the provincial scale was applicable for pixel-scale at the spatial resolution of 0.125 arc-degree. Quantitative biases might be introduced while directly transferring the regression relationship between different spatial scales. To correct this bias, we applied an adjustment to retain the total volume of pixel-level water footprint within a province identical to that of the provincial-level using the following Equation:

$$WF_i = \frac{W\hat{F}_P}{\sum_{i \in P} W\hat{F}_i} \times W\hat{F}_i \quad (15)$$

where $W\hat{F}_i$ denotes the future pixel-level fitted water footprint at pixel i that belongs to province P ; $W\hat{F}_P$ denotes the future provincial-level fitted water footprint for the entire province P ; $W\hat{F}_i$ denotes the future fitted water footprint at pixel i ; and the WF_i denotes the calibrated water footprint at pixel i . Though the above regression and adjustment, future patterns of water footprint were expected to be projected, with both reasonable water footprint amount within the administrative unit and extra spatial detail at the spatial resolution of 0.125 arc-degree.

The future population data were derived based on NCAR population projection. For better accounting for the future projection of population in China, this dataset was subset at the China region and was adjusted based on the ratio of population acquired from the Chinese Statistical Yearbook to the NCAR population projection at the initial year (2000):

$$pop_{SSP}^{2050} = \text{ratio}_{NCAR/YB}^{2000} \times pop_{NCAR}^{2050} \quad (16)$$

where pop_{SSP}^{2050} is the adjusted population in 2050 under different SSP scenarios; $\text{ratio}_{NCAR/YB}^{2000}$ is the adjusted ratio estimated according to population statistics acquired from the Chinese Statistical Yearbook and the NACR population projection in 2000; and the pop_{NCAR}^{2050} is the projected population in 2050 from the NCAR dataset under different SSP scenarios.

The future urbanization rate was obtained from the projected urban and rural population in the NCAR dataset, according to the definition of ratio of urban population to the total population within the administrative unit:

$$ur = \frac{pop_u}{pop_u + pop_r} \times 100\% \quad (17)$$

where ur is the estimated urbanization rate; and pop_u and pop_r are, respectively, the urban and rural population aggregated from the adjusted NCAR population within the administrative unit. All cells within the administrative unit share the same urbanization rate.

4. Results and discussion

4.1. Historical water footprint accounting

Historical water footprints at the provincial scale in 2007, 2010, and

Table 1

Coefficients and *p*-values of the water footprint regression with $\alpha = 0.05$ ($R^2 = 0.784$).

Variable	Coefficient	<i>p</i> -Value
Population	0.637	0.000**
Urbanization rate	0.631	0.000**
Built-up area	0.110	0.037**
Constant	-1.797	0.000**

2012 were accounted using a 30-region 30-sector MRIO model described in Section 3.1. We then aggregated 30 sectoral water footprint consumptions to derive provincial water footprint of 30 provinces as well as their change trends in these three years (Fig. 1 and Supplementary Table S2). According to the results, water footprint volume of China increased by 35.5% from 2007 (268.81 billion m³) to 2012 (364.25 billion m³). With a few exceptions (Shanghai and Gansu), most provinces show an increasing trend during this period. This is mainly due to the rapid increase of socioeconomic activities and urbanization process during this period (Zhang and Anadon, 2014; Zhang et al., 2018). Among these provinces, Hebei has the largest growth volume of 12.72

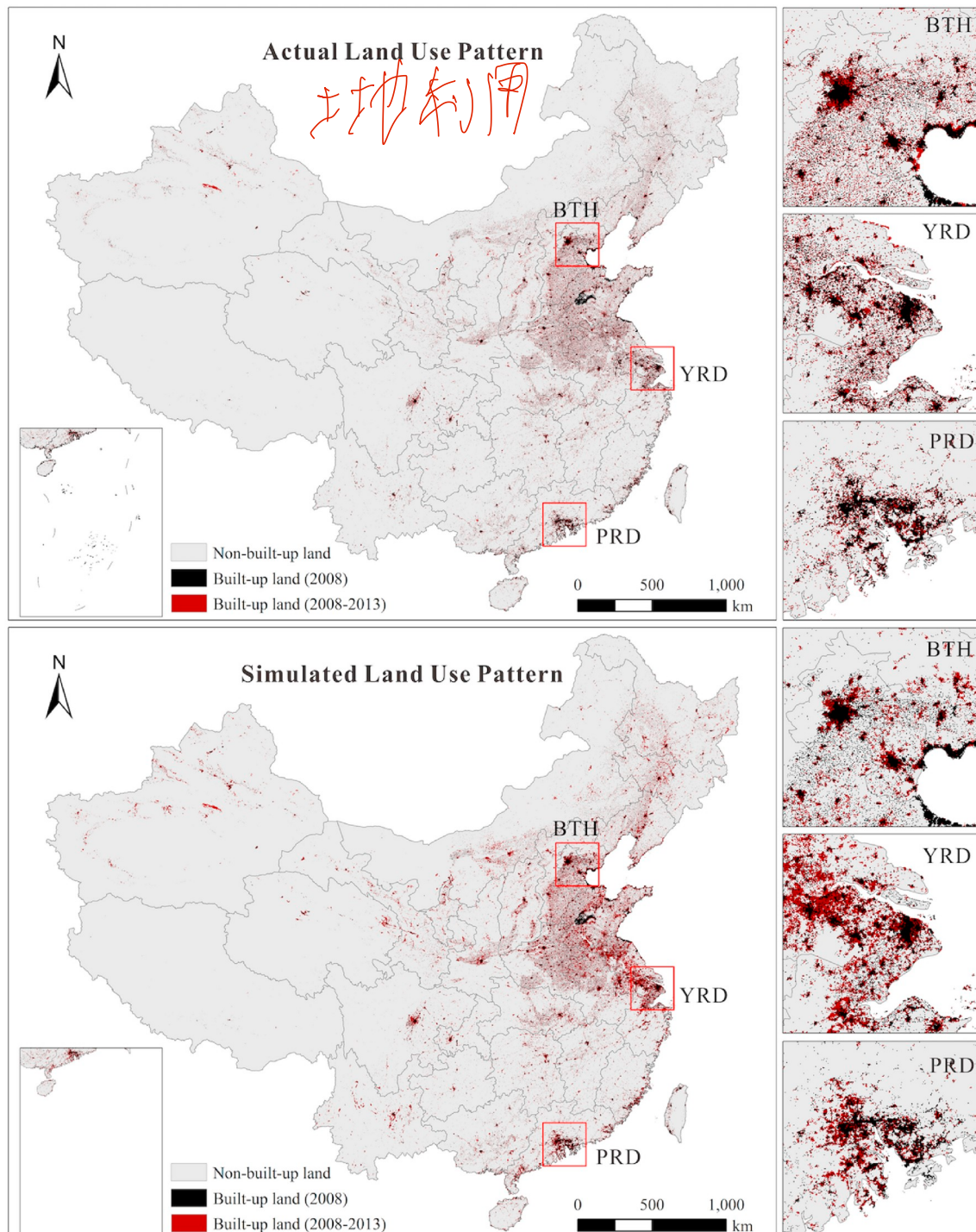


Fig. 2. Actual (top) and simulated (bottom) built-up land patterns of China in 2013.

billion m³ (137.6%), and Inner Mongolia has the greatest growth rate of 198.4% (7.39 billion m³). In 2012, the top five provinces consumed more than 30% of water footprint volume of entire China, including Jiangsu (7.54%, 27.46 billion m³), Guangdong (6.65%, 24.22 billion m³), Hebei (6.03%, 21.96 billion m³), Xinjiang (5.68%, 20.69 billion m³), and Sichuan (5.36%, 19.54 billion m³).

Spatial distributions and variations of provincial water footprint for 2007, 2010, and 2012 were shown in [Supplementary Figs. S2, S3, and S4](#), respectively. Overall, coastal provinces in east and south China, especially Shandong, Jiangsu, and Guangdong, consumed much larger water footprints in 2007 than the inner and northern provinces such as Qinghai, Ningxia, Shanxi, and Inner Mongolia. Even though a similar increasing trend was observed for most provinces, the growth rates in central provinces were obviously slower than that in the eastern provinces (Heilongjiang, Hebei, and Zhejiang) for 2007–2012. One potential reason is that, suggested by [Deng et al. \(2016\)](#), a great number of populations in the northwest and central provinces were moving to the eastern coastal regions for better job opportunity. Two exceptions were Xinjiang and Shanghai. Xinjiang, which is in northwest China, consumed a considerable volume of water footprint and the volume increased rapidly from 9.93 billion m³ in 2007 to 19.54 billion m³ in 2012. On the contrary, the water footprint in Shanghai decreased slightly from 14.23 billion m³ to 11.34 billion m³ during the same period.

4.2. Analysis of drivers of water footprint

The drivers of water footprint were identified according to the regression analysis described in Section 3.3. Here, we only presented the regression model in which all independent variables pass the significance test with a significance level of $\alpha = 0.05$; for the remaining trial results, please refer to the [Supplementary Tables S3–S5](#). The final adopted regression consists of three independent variables, e.g., population urbanization rate, and built-up land area. The regression coefficients and p -values were summarized in [Table 1](#). The regression analysis yields a coefficient of determination $R^2 = 0.784$ ([Supplementary Fig. S5](#)), suggesting a promising agreement between the fitted water footprint and that derived based on the MRIO analysis.

The coefficients of population and urbanization rate (~0.63) are relatively larger than that of the built-up land area (~0.11), suggesting more dominant roles in the regression for fitting the water footprint. Substituting the regression coefficients in [Table 1](#) into Equation (14), we obtain the following regression model for future water footprint under different SSP scenarios:

$$\log_{10}(\widehat{WF}) = 0.637 \times \log_{10}(pop) + 0.631 \times \log_{10}(ur) + 0.110 \times \log_{10}(bu) - 1.797 \quad (18)$$

where the \widehat{WF} is the projected water footprint; pop is the future population; ur is the future urbanization rate; and bu is the future built-up land area.

4.3. Built-up land simulation and validation

As we described in [Methodology](#) section, the simulation model was tested by simulating the historical period of 2008–2013 before its application for future built-up land simulation. The suitability of each 1 × 1 km² land patch to develop into built-up land was calibrated using the BP-ANN model (see [Supplementary Fig. S6](#)) based on the topographic factors and socio-economical drivers. Then that state of each land patch evolves according to the transformation probability estimated using Equation (10) and the roulette selection mechanism described in Section 3.2. We present the actual (top panel of [Fig. 2](#)) and simulated (bottom panel of [Fig. 2](#)) patterns of built-up land in 2013 to show a visual comparison at national scale. Besides, enlargements in

Table 2

Indicator of FoM of the simulated built-up land pattern in 2013.

Region	FoM
Entire China	0.29
Beijing-Tianjin-Hebei (BTH)	0.30
Yangtze River Delta (YRD)	0.26
Pearl River Delta (PRD)	0.28

Table 3

Demand projections of future built-up land under different SSP scenarios (thousand km²).

Year	SSP1	SSP2	SSP3	SSP4	SSP5
2020	280.52	258.03	237.47	280.05	281.95
2030	335.84	284.34	245.45	333.43	335.82
2040	340.13	267.12	217.37	333.99	340.14
2050	310.56	226.68	205.11	299.73	310.66

three metropolitan regions, i.e., Beijing-Tianjin-Hebei (BTH), Yangtze River Delta (YRD), and Pearl River Delta (PRD) were also illustrated to show local agreement between simulated and actual patterns (right panels of [Fig. 2](#)). Areas with black color represent built-up land that existed prior to 2008, and land patches with red color represent the newly developed built-up land during 2008–2013 period. In general, the simulated pattern agrees well with the actual pattern at the national scale. New developments of built-up land patches mostly emerge around exiting urban areas.

To quantitatively evaluate the simulation, we adopted the indicator of ‘Figure of Merit’ (FoM) to evaluate the performance of simulation ([Pontius et al., 2008](#)). The FoM indicator focuses on the change prediction rather than the overall pattern agreement, thus avoiding biases introduced by the persistent non-changed areas in traditional assessment metrics, such as overall accuracy and Kappa coefficient. The FoM values at the national scale and three rapidly developing metropolitan areas where the emerged build-land developments are mainly distributed are summarized in [Table 2](#). The FoM of entire China is 0.29 and varies from 0.26 to 0.30 for different metropolitan areas. According to recent studies on urban simulation models, a range of FoM values between 0.10 and 0.30 have been reported at different spatial scales ([Chen et al., 2014; Liu et al., 2017; Thapa and Murayama, 2011](#)). Therefore, our simulation achieved similar and even slightly better performance than those reported previously, indicating that it is effective for future built-up land simulation under different SSP scenarios.

4.4. Future built-up land and water footprint simulation

4.4.1. Future built-up land simulation

The future demand of built-up land under different SSP scenarios were projected via a MRIO analysis following the methodology proposed in [Chen et al. \(2019\)](#). According to the projections ([Table 3](#)), the volume of built-up land demand varies under different SSP scenarios. The demand is the largest under SSP1 and SSP5 (310 thousand km²), and the smallest under SSP3 (205 thousand km²). Overall, the built-up land projected to increase and reach a peak during the 2030s (SSP2 and SSP3) and 2040s (SSP1, SSP4 and SSP5), and decline after 2040 due to the shrinking population. Note that the transitions from natural to built-up land are usually considered to be irreversible. Thus, the built-up demands in the simulation process were set to be maximum urban expansion during the 2030s and 2040s.

The calibrated simulation model was applied to project the future built-up land pattern from 2010 to 2050 under different SSP scenarios at the given demands listed in [Table 3](#). The simulated patterns in 2050 under the five SSP scenarios are presented in [Supplementary Figs. S7–S11](#). Enlargements of the future simulations at the Yangtze

一下

让我写写感受

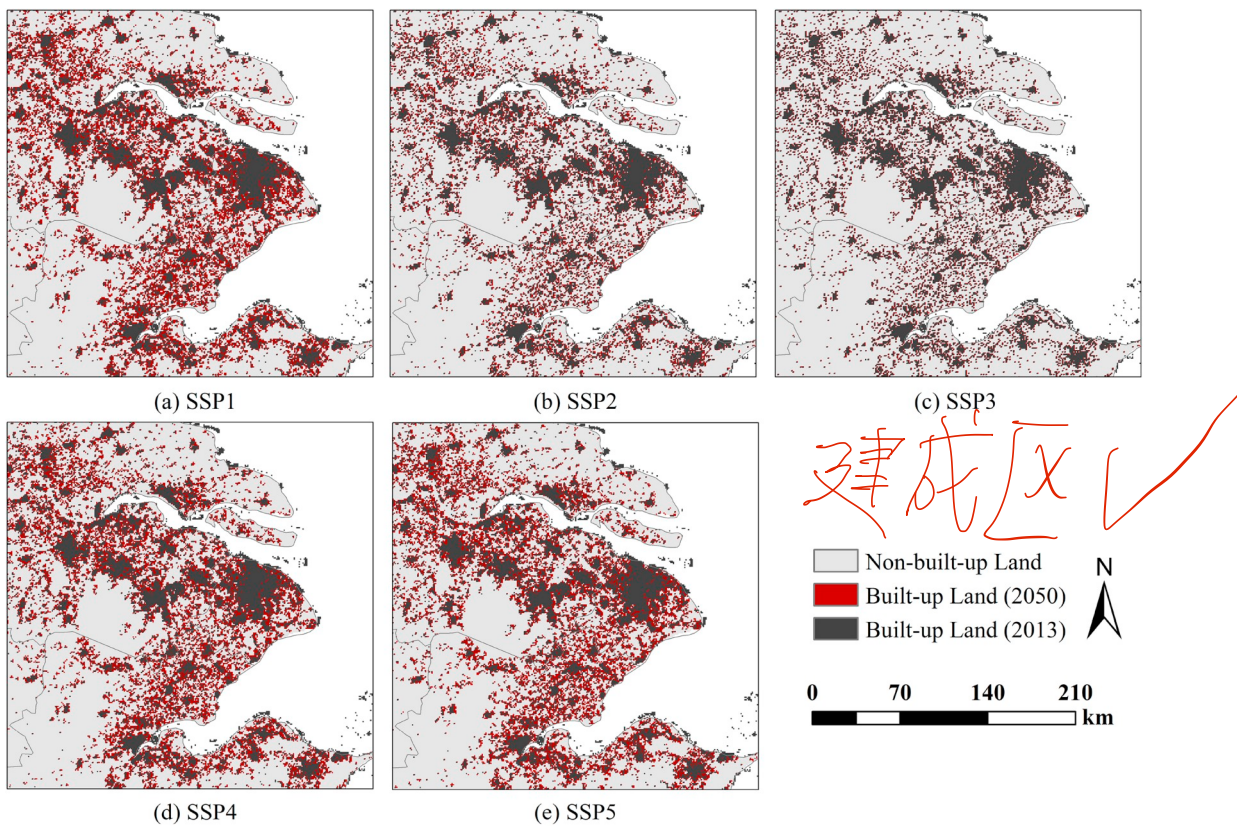


Fig. 3. Enlargements of simulated built-up land patterns in 2050 under the five SSP scenarios.

Table 4

Population of typical provinces in 2050 under the SSP scenarios (million).

Province	2010	2050				
		SSP1	SSP2	SSP3	SSP4	SSP5
Guangdong	104.41	101.07	99.90	98.50	97.91	101.10
Shandong	95.88	95.68	97.69	100.07	92.44	95.64
Henan	94.05	92.87	95.14	97.82	89.68	92.81
Jiangsu	78.69	76.57	77.67	79.02	74.00	76.50
Xinjiang	21.85	16.69	17.69	18.78	16.16	16.74
Hainan	8.69	6.69	7.03	7.41	6.47	6.70
Ningxia	6.33	5.22	5.49	5.79	5.04	5.23
Qinghai	5.63	4.06	4.39	4.75	3.92	4.07
Entire China	1330.85	1235.58	1274.26	1318.53	1194.17	1235.70

River Delta metropolitan region under five SSP scenarios are illustrated in Fig. 3 to show the spatial specificity and difference among the scenarios. As expected, a plenty of new built-up land patches were projected to develop around the existing urban areas under the SSP5 and SSP1 scenarios which were designed to be pathways characterized by rapid development. On the contrary, limited amount of newly developed built-up lands were simulated in the SSP3 scenario. The area of built-up land in some typical provinces in 2050 under different SSP scenarios is presented in Supplementary Table S6; the average growth rates of simulated built-up area within these provinces are given in the last column of the table. According to the results, eastern provinces such as Anhui, Henan, Shandong, and Hebei, account for the majority of newly-developed built-up land. The average growth rate of these provinces (43–61%) are much higher than the average level of entire China (32.38%).

4.4.2. Future water footprint projection

4.4.2.1. Population adjustment. We applied the linear adjustment using

Equation (16) to each grid of the NACR projected population in China. The ratio is estimated to be 1.0185 in this case. The adjusted population patterns in 2050 under different SSP scenarios are presented in Supplementary Fig. S12. In general, cities along the eastern coastline and the East China Plain are densely populated. At national scale, no significant visual differences were observed in the broad pattern among the five SSP scenarios, probably because that China has a huge population base and the differences among scenarios are not comparable. We summarize the aggregated population statistics at provincial scales (Table 4), including four provinces with largest population (Guangdong, Shanghai, Henan, and Jiangsu) and four provinces with smallest population (Xinjiang, Hainan, Ningxia, and Qinghai). From the table, widespread population decline can be observed across most cities of China in all SSP scenarios. This result is in line with those of the previous studies (Jones and O'Neill, 2016; Liu et al., 2010), suggesting a substantial decline in rural population and a relatively stable urban population in the future.

4.4.2.2. Urbanization rate. We estimated the future urbanization rate

Table 5

Summary of urbanization rate (%) of provinces under different SSP scenarios.

Province	2010	2050				
		SSP1	SSP2	SSP3	SSP4	SSP5
Shanghai	89	100	100	98	100	89
Tianjin	80	100	92	79	100	80
Shandong	50	100	95	84	100	50
Jiangsu	61	100	98	94	100	61
Henan	43	97	91	81	97	43
Yunnan	35	37	22	17	37	35
Qinghai	45	36	28	26	36	45
Gansu	37	34	21	17	34	37
Xinjiang	43	28	24	21	29	43
I. Mongolia	89	100	100	98	100	89
Entire China	80	100	92	79	100	80

from the projected urban and rural population in the NCAR dataset, based on the ratio of urban population to the total population within the local administrative units (i.e., districts and counties). The estimated patterns of the urbanization rate under different SSP scenarios are presented in [Supplementary Fig. S13](#). Widespread urbanization is expected to occur under all SSP scenarios, especially under the SSP1 and SSP5 that are characterized by rapid development. Urbanization was projected to be the most conservative under the SSP3 scenario, which is characterized by localized land policies for mitigation and slow development for adaptation.

We summarized the estimated future urbanization rate of the top five and last five urbanized provinces of China in [Table 5](#). The urbanization rate of these provinces in 2010 are also attached in the table. According to the results, the average urbanization rate of entire China is expected to reach 80% in 2050 under the SSP1, SSP4, and SSP5 scenarios, but is still below 60% under the SSP3 scenario. Provinces along the eastern coastline (e.g., Shanghai, Tianjin, Shandong, and Jiangsu) and the North China Plain (e.g., Henan) are projected to be at nearly 100% urbanization rate under the three rapid development scenarios of SSP1, SSP4, and SSP5. However, counter-urbanization was observed among the

provinces in the northwest dryland (e.g., Qinghai, Gansu, Xinjiang, and Inner-Mongolia) and southwest regions (Yunnan). Urbanization rate of these provinces are projected to decrease by 20–30% by 2050.

4.4.2.3. Future water footprint projection. The future water footprint patterns under the five SSP scenarios were projected according to the regression presented in [Equation \(18\)](#) at both pixel-level and provincial-level. The projected pixel-scale results were then adjusted according to the quantitative constrain using [Equation \(15\)](#). We present the adjusted pixel-level water footprint patterns at national scale under the five SSP scenarios ([Fig. 4](#)). The future patterns of provincial water footprint can be found in the [Supplementary Figs. S14–S18](#). Overall, it appears that, at the national scale, the projected water footprint shares a similar pattern under all the SSP scenarios. The hotspots of water footprint (red color) are projected to locate at provinces and cities along the eastern coastline. Another hotspot was found around the cities in the Sichuan Basin (Sichuan Province and Chongqing City). On the contrary, the water footprint volume in most northern and western provinces appears to be negligible. Most of land grids in these areas are projected to have nearly zero water footprint due to their very low population density ([Jones and O'Neill, 2016](#)). This strong spatial heterogeneity among eastern coastal regions and northwestern inland provinces probably results from China's unbalanced development ([Zhang and Anadon, 2014](#)) in the future SSP scenarios, as the projected water footprint volumes are based on the selected socioeconomic-related variables. The majority of future population will be thickly settled on the highly urbanized cities in eastern provinces of China ([Jones and O'Neill, 2016](#)), and therefore consume a great portion of water footprint. By contrast, population growth and urbanization rate in northwest China are expected to stagnate and even decline in the future ([Supplementary Figs. S12 and S13](#)), resulting in small water footprint projection in these regions.

In order to quantitatively investigate the future water footprint, we aggregated and summarized the volume of provincial water footprint in 2050 under the five SSP scenarios. Summaries of ten typical provinces, including the five largest water footprint provinces (Shandong, Henan,

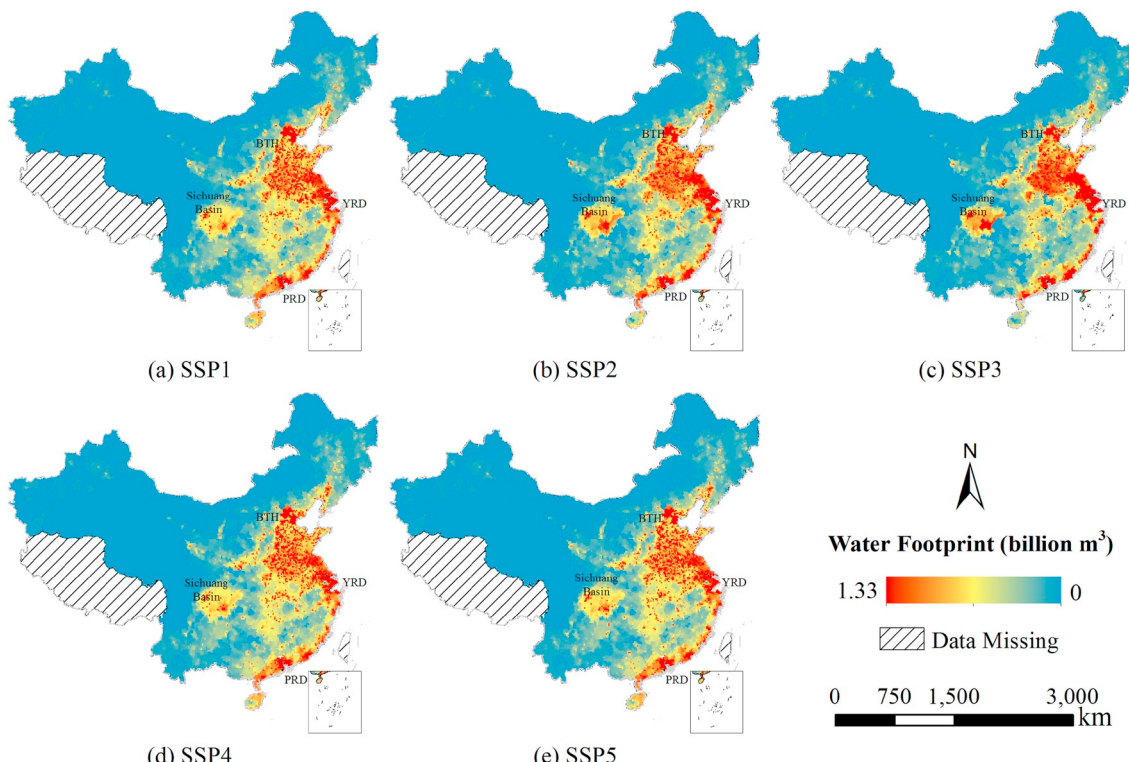
**Fig. 4.** Projected water footprint of China in 2050 under the SSP scenarios.

Table 6
Provincial water footprint in 2050 under the SSP scenarios (billion m³).

Province	2010	2050				
		SSP1	SSP2	SSP3	SSP4	SSP5
Shandong	14.68	32.04	30.66	28.27	31.33	32.03
Henan	13.27	30.88	28.58	26.57	30.18	30.84
Guangdong	20.20	28.73	26.87	24.32	28.12	28.78
Jiangsu	24.18	27.56	26.49	25.57	26.98	27.54
Hebei	9.57	24.70	23.74	20.86	24.29	24.73
Gansu	7.45	5.05	3.89	3.53	4.94	5.05
Xinjiang	13.41	4.00	3.74	3.65	3.92	4.00
Hainan	1.75	3.71	2.41	1.72	3.61	3.71
Ningxia	2.11	1.93	1.69	1.45	1.89	1.93
Qinghai	2.47	1.58	1.42	1.42	1.55	1.58
Entire China	290.35	396.53	357.06	318.58	387.02	396.54

Guangdong, Jiangsu, and Hebei) and the five smallest water footprint provinces (Gansu, Xinjiang, Hainan, Ningxia, and Qinghai), are listed in Table 6. Besides, provincial water footprint in 2010 is also provided in the table. We can observe that the volume of China's water footprint increases to varying magnitudes under the SSP scenarios. In the SSP1, SSP4 and SSP5 scenarios, it is projected to reach up to nearly 400 billion m³, almost 40% increase compared to that in 2010. Similar to the national tendency under all scenarios, the water footprints of top five provinces are expected to increase. In particular, water footprint in the provinces of Shandong, Henan and, Hebei were projected to increase dramatically. The increase in these three provinces ranges from 100 to 130%, probably due to the massive population expansion toward the

end of 2050. On the contrary, water footprints of the bottom five provinces are projected to decrease with only one exception (Hainan). One possible explanation is that, as suggested in Table 4, the populations of these western provinces would probably migrate to the central and eastern provinces. Due to relatively slow development, water footprint consumption in SSP3 is projected to be the smallest among all SSP scenarios.

To show the spatial pattern details and the differences in water footprint under the five SSP scenarios, enlargements of several metropolitan areas are presented (Fig. 5), including BTH (top panel), YRD (middle panel), and PRD (bottom panel). We applied a discrete classified colormap with a higher contrast to these enlargements to outline the local spatial heterogeneity. From these three figures we observed that, despite the quantitative differences among the five SSP scenarios (Table 6), the water footprint in these metropolitan areas share similar spatial patterns for the different scenarios. In the BTH metropolitan area, the hotspots of water footprint are projected to aggregate around the city center of the Beijing and Tianjin, whereas in the Hebei province the projected patterns are rather dispersive under all the SSP scenarios. As to the YRD metropolitan area, Shanghai dominates the water footprint in this region under all the SSP scenarios. Most areas within the Shanghai administrative boundary are projected to possess a massive volume of water footprint, up to 0.4 billion m³ per 0.125 arc-degree grid cell. Jiangsu province accounts for the largest portion (~50% under all the SSP scenarios) of water footprint in the YRD region. Rather than aggregated in capital city, the water footprint in the Jiangsu province is scattered around local cities, probably due a relatively balanced future

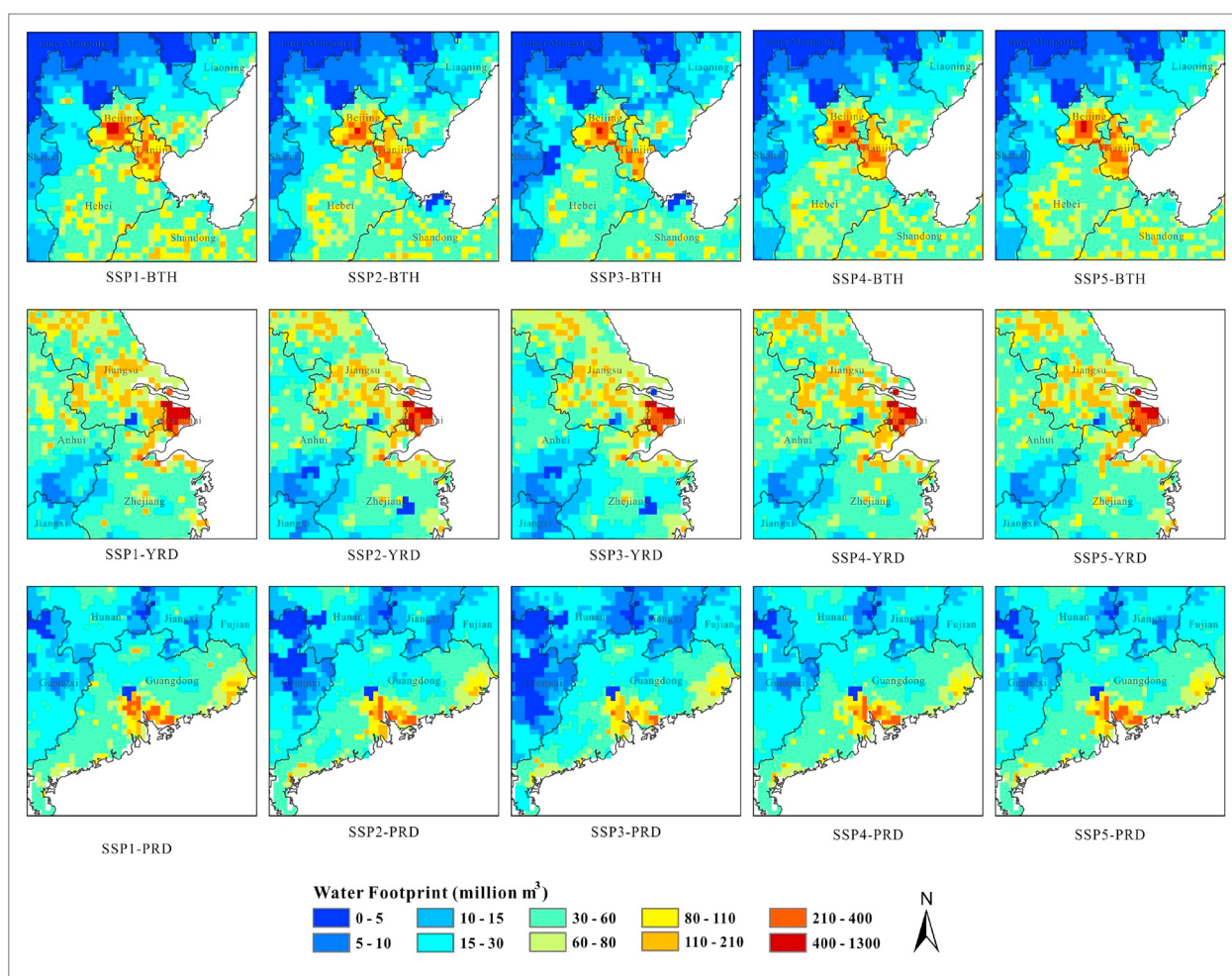


Fig. 5. Projected water footprint pattern in 2050 under the SSP scenarios in metropolitan areas of BTH (top panel), YRD (middle panel), and PRD (bottom panel).

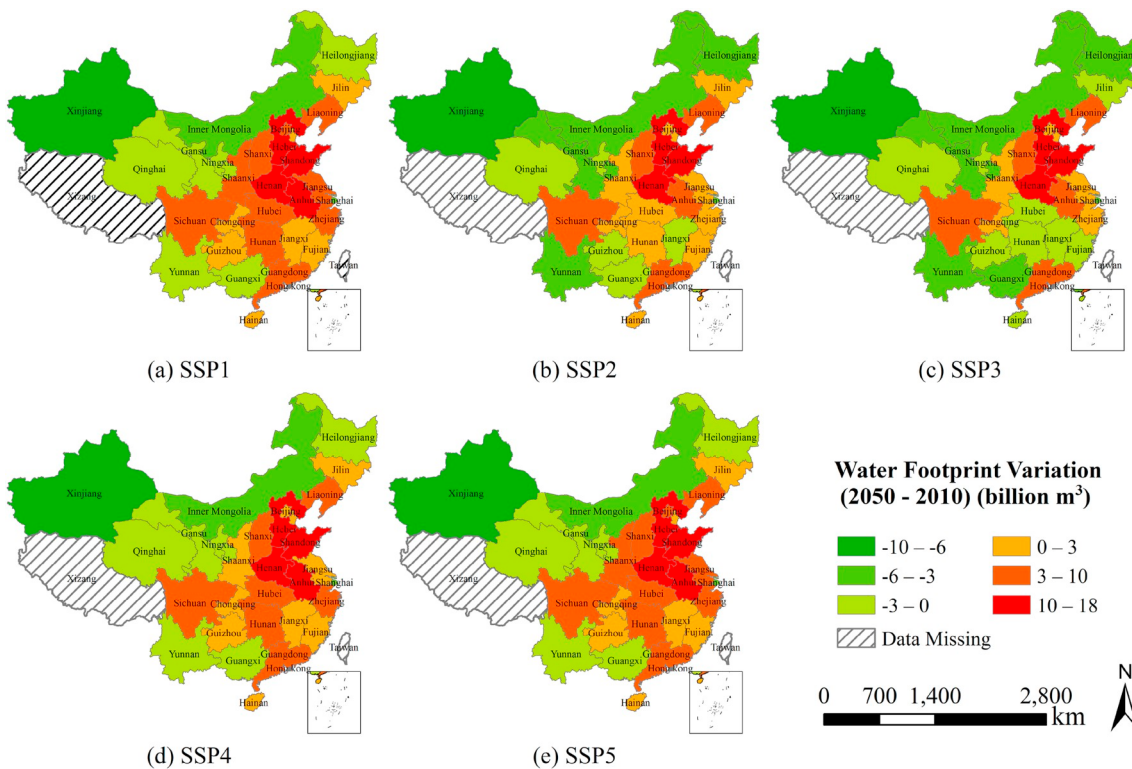


Fig. 6. Provincial water footprint Changes between 2050 and 2010 under the SSP scenarios.

development within the province. In the PRD region, the hotspots of water footprint under all SSP scenarios are projected to be located in the cities around the Pearl River estuary (Guangzhou, Dongguan and Shenzhen). In addition, a secondary hotspot is found in the eastern part of Guangdong province. No obvious differences were observed among the five SSP scenarios.

To investigate the changes in spatial patterns of future water footprint among the different scenarios, we present Fig. 6 to show the differences in provincial water footprint between 2050 and that of 2010 under the five SSP scenarios. We can observe that in the future, water footprint consumption in most of the eastern provinces are projected to increase by different magnitudes. Increase in provinces of Hebei, Shandong, and Henan are the most significant (up to 18 billion m³) under all the SSP scenarios. Contrasting situations are observed in the northern and western provinces, most of which show decreases by more than 3 billion m³. The Sichuan province will likely to account for a significant increase even though it is in southwest China. Unexpected changes were found in Shanghai where the future water footprint will decrease by approximately 5 billion m³ under all the SSP scenarios. Even though most provinces show a consistent tendency under the SSP scenarios, we observe that some lesser-developed provinces, such as Guizhou and Jiangxi, are projected to increase by 0–3 billion m³ under SSP1, SSP4 and SSP5 scenarios, whereas the decrease is by 0–3 billion m³ under SSP2 and SSP3 scenarios. Provinces of Hubei and Hunan also show inconsistent tendency under different scenarios, which are projected to decrease only under SSP3 by 0–3 billion m³, but increase under other SSP scenarios by 0–10 billion m³.

The analysis presented in this study has several limitations. First, the input-output table data (2007, 2010, and 2012) used in the analysis cannot reflect the latest picture of China's inter-provincial water flows, even though the latest data of 2014 were published recently. We will address this issue in the future by incorporating more updated data for better projection of future water footprint. Second, in order to obtain spatial heterogeneity of future water footprint pattern, we assumed the same regression among the provincial and the 0.125 arc-degree pixel

scales. Even though we applied an adjustment to retain the total volume of pixel-level water footprint within a province identical to that of the provincial-level, biases might still be introduced while directly transferring the regression relationship between different spatial scales. Third, the projected future water footprint is an aggregation of multiple sectors, while future water footprint patterns of specific sectors (e.g., agricultural sector, industrial sector) will be more valuable for effective water management policies to mitigate water resource scarcity and inequality. In future study, we will incorporate complementary data and models to project future water footprint of specific sectors.

5. Conclusion

In this study, we present an approach that is capable of projecting future water footprint patterns of China at a **fine resolution** under the SSP scenario framework. The core idea of the projection approach is an extrapolation from historical relationship between water footprint consumption accounted by the MRIO analysis and the drivers identified using the regression analysis. The simulation of future built-up land patterns under the different SSP scenarios are crucial to the future water footprint projections. MRIO analysis-based projection of future built-up land demand under SSP scenarios was performed, after which, the local evolution of land use change was simulated using the FLUS model, taking into account the land use suitability, local autocorrelation effect, and multiple land use competition during the evolution process.

Based on the presented approach, we found that the accounted historical water footprint of China increased dramatically by 35.5% from 2007 (268.81 billion m³) to 2012 (364.25 billion m³), and the coastal provinces in east China consumed the most of them. The built-up land area, urbanization rate, and population were identified as the valid drivers (p -value < 0.05) of the water footprint consumption with a determination coefficient $R^2 = 0.784$. The future built-up land demands of China were projected to increase and reach a peak during the 2030s and 2040s (approximately 340 thousand km² under SSP1, SSP4 and SSP5, and 250 thousand km² under SSP2 and SSP3). To meet these

future built-up land demands, the future patterns of built-up land at spatial resolution of $1 \times 1 \text{ km}^2$ were simulated. Results suggest that eastern provinces account for the majority of newly developed built-up land under all SSP scenarios.

The future water footprint patterns of China at spatial resolution of 0.125 arc-degree were projected by the multi-variable regression on the derived patterns of built-up land, urbanization rate, and population. The projected future water footprint patterns were adjusted by the provincial volume constraint. The results suggest that the volume of China water footprint in 2050 increases by various magnitudes under alternative SSP scenarios. Under the SSP1, SSP4 and SSP5 scenarios, the water footprint consumptions are projected to reach up to a total volume of nearly 400 billion m^3 in 2050, almost 40% increase compared to that in 2010. Water footprint consumption under the SSP3 scenario is 318.58 billion m^3 (9.72% increase), the smallest compared with all other SSP scenarios. Spatially, water footprint consumption in the eastern provinces (Shandong, Henan and Hebei) will increase dramatically by 100–130% under all SSP scenarios, while that in the western provinces (Xinjiang, Ningxia, and Qinghai) will significantly decrease. Despite different magnitudes under the SSP scenarios, the water footprints share very similar spatial patterns at the local pixel scale among the scenarios in the three greatest metropolitan areas of China: BHT, YRD, and PRD. Water footprints in lesser-developed provinces of southern China (Jiangxi, Guizhou, Hunan, and Hubei) are projected to increase under rapid development scenarios (SSP1, SSP4, and SSP5), but decrease under slow development scenarios (SSP2 and SSP3). These water footprint results suggest a more severe water scarcity situation in the future from a consumption-oriented perspective. The challenge is attributed to not only the increased total water consumption but also to the more uneven spatial distribution of water footprint under alternative SSP scenarios. More effective water management policies and measures are urgently needed to mitigate future water resource scarcity and inequality.

Acknowledgement

We sincerely thank the anonymous reviewers for their useful comments and suggestions. Y. Zhang is grateful to Penghua Liu for his kind help and support throughout this research. This research was supported by the National Key R&D Program of China (2017YFA0604402), the National Natural Science Foundation of China (Grant No. 41871306), the Key National Natural Science Foundation of China (Grant No. 41531176), the China Postdoctoral Science Foundation (Grant No. 2018M633227), and the research fund from Shenzhen Key Laboratory of Spatial Smart Sensing and Service.

Appendix A. Supplementary data

Supplementary data to this article can be found online at <https://doi.org/10.1016/j.jenvman.2020.110102>.

Authors' contributions

X. Xu and Y. Zhang contributed equally to this work; Y. Chen designed the research; Y. Zhang and X. Xu performed experiments and computational analysis; X. Xu drafted the manuscript; X. Xu and Y. Chen amended the manuscript.

References

- Aerts, J.C.J.H., Heuvelink, G.B.M., 2002. Using simulated annealing for resource allocation. *Int. J. Geogr. Inf. Sci.* 16, 571–587.
- Allan, J.A., 1998. Virtual water: a strategic resource global solutions to regional deficits. *Gr. Water* 36, 545–546.
- Batty, M., 1997. Cellular automata and urban form: a primer. *J. Am. Plan. Assoc.* 63, 266–274.
- Burek, P., Satoh, Y., Fischer, G., Kahil, M.T., Scherzer, A., Tramberend, S., Nava, L.F., Wada, Y., Eisner, S., Flörke, M., 2016. Water Futures and Solution: Fast Track Initiative. International Institute for Applied Systems Analysis (IIASA), Laxenburg, Austria.
- Chapagain, A.K., Hoekstra, A.Y., Savenije, H.H.G., Gautam, R., 2006. The water footprint of cotton consumption: an assessment of the impact of worldwide consumption of cotton products on the water resources in the cotton producing countries. *Ecol. Econ.* 60, 186–203.
- Chen, Y.M., Li, X., Liu, X.P., Ai, B., 2014. Modeling urban land-use dynamics in a fast developing city using the modified logistic cellular automaton with a patch-based simulation strategy. *Int. J. Geogr. Inf. Sci.* 28, 234–255.
- Chen, Y.M., Li, X., Liu, X.P., Ai, B., Li, S.Y., 2016. Capturing the varying effects of driving forces over time for the simulation of urban growth by using survival analysis and cellular automata. *Landsc. Urban Plan.* 152, 59–71.
- Chen, Y.M., Li, X., Liu, X.P., Zhang, Y.Y., Huang, M., 2019. Tele-connecting China's future urban growth to impacts on ecosystem services under the shared socioeconomic pathways. *Sci. Total Environ.* 652, 765–779.
- Clarke, K.C., Gaydos, L.J., 1998. Loose-coupling a cellular automaton model and GIS: long-term urban growth prediction for San Francisco and Washington/Baltimore. *Int. J. Geogr. Inf. Sci.* 12, 699–714.
- Deng, G.Y., Ma, Y., Li, X., 2016. Regional water footprint evaluation and trend analysis of China-based on interregional input-output model. *J. Clean. Prod.* 112, 4674–4682.
- Dietzel, C., Clarke, K.C., 2007. Toward optimal calibration of the SLEUTH land use change model. *T. GIS* 11, 29–45.
- Dietzenbacher, E., Velazquez, E., 2007. Analysing Andalusian virtual water trade in an input-output framework. *Reg. Stud.* 41, 185–196.
- Feng, K.S., Hubacek, K., Pfister, S., Yu, Y., Sun, L.X., 2014. Virtual scarce water in China. *Environ. Sci. Technol.* 48, 7704–7713.
- Feng, L., Chen, B., Hayat, T., Alsaedi, A., Ahmad, B., 2017. The driving force of water footprint under the rapid urbanization process: a structural decomposition analysis for Zhangye city in China. *J. Clean. Prod.* 163, S322–S328.
- Gerbens-Leenes, P.W., Mekonnen, M.M., Hoekstra, A.Y., 2013. The water footprint of poultry, pork and beef: a comparative study in different countries and production systems. *Water Resources and Industry* 1, 25–36.
- Guan, Q.F., Shi, X., Huang, M.Q., Lai, C.G., 2016. A hybrid parallel cellular automata model for urban growth simulation over GPU/CPU heterogeneous architectures. *Int. J. Geogr. Inf. Sci.* 30, 494–514.
- Han, M.Y., Chen, G.Q., Li, Y.L., 2018. Global water transfers embodied in international trade: tracking imbalanced and inefficient flows. *J. Clean. Prod.* 184, 50–64.
- Hawkins, J., Ma, C.B., Schilizzi, S., Zhang, F., 2015. Promises and pitfalls in environmentally extended input-output analysis for China: a survey of the literature. *Energy Econ.* 48, 81–88.
- He, C.Y., Zhao, Y.Y., Tian, J., Shi, P.J., 2013. Modeling the urban landscape dynamics in a megalopolitan cluster area by incorporating a gravitational field model with cellular automata. *Landsc. Urban Plan.* 113, 78–89.
- Hoekstra, A., Hung, P.Q., 2003. Virtual water trade: a quantification of virtual water flows between nations in relation to international crop trade. In: Proceedings of the International Expert Meeting on Virtual Water Trade 12. UNESCO-IHE Institute for Water Education, Delft, The Netherlands, pp. 25–47.
- Hoekstra, A.Y., Mekonnen, M.M., 2012. The water footprint of humanity. *Proc. Natl. Acad. Sci. U.S.A.* 109, 3232–3237.
- Jia, P., Qiu, Y.L., Gaughan, A.E., 2014. A fine-scale spatial population distribution on the high-resolution gridded population surface and application in alachua county, Florida. *Appl. Geogr.* 50, 99–107.
- Jiang, Y., 2009. China's water scarcity. *J. Environ. Manag.* 90, 3185–3196.
- Jones, B., O'Neill, B.C., 2016. Spatially explicit global population scenarios consistent with the Shared Socioeconomic Pathways. *Environ. Res. Lett.* 11, 084003.
- Kocabas, V., Dragicevic, S., 2006. Assessing cellular automata model behaviour using a sensitivity analysis approach. *Comput. Environ. Urban* 30, 921–953.
- Lenzen, M., Moran, D., Bhaduri, A., Kanemoto, K., Bekchanov, M., Geschke, A., Foran, B., 2013. International trade of scarce water. *Ecol. Econ.* 94, 78–85.
- Letourneau, A., Verburg, P.H., Stéhfest, E., 2012. A land-use systems approach to represent land-use dynamics at continental and global scales. *Environ. Model. Softw.* 33, 61–79.
- Li, X., Chen, G.Z., Liu, X.P., Liang, X., Wang, S.J., Chen, Y.M., Pei, F.S., Xu, X.C., 2017. A new global land-use and land-cover change product at a 1-km resolution for 2010 to 2100 based on human-environment interactions. *Ann. Assoc. Am. Geogr.* 107, 1040–1059.
- Li, X., Yeh, A.G., 2002. Neural-network-based cellular automata for simulating multiple land use changes using GIS. *Int. J. Geogr. Inf. Sci.* 16, 323–343.
- Li, X., Yeh, A.G.-O., 2000. Modelling sustainable urban development by the integration of constrained cellular automata and GIS. *Int. J. Geogr. Inf. Sci.* 14, 131–152.
- Li, X., Zhang, X.H., Yeh, A., Liu, X.P., 2010. Parallel cellular automata for large-scale urban simulation using load-balancing techniques. *Int. J. Geogr. Inf. Sci.* 24, 803–820.
- Lin, C., Suh, S., Pfister, S., 2012. Does south-to-north water transfer reduce the environmental impact of water consumption in China? *J. Ind. Ecol.* 16, 647–654.
- Liu, J.G., Yang, W., 2012. Water sustainability for China and beyond. *Science* 337, 649–650.
- Liu, J.G., Zang, C.F., Tian, S.Y., Liu, J.G., Yang, H., Jia, S.F., You, L.Z., Liu, B., Zhang, M., 2013. Water conservancy projects in China: achievements, challenges and way forward. *Glob. Environ. Chang.* 23, 633–643.
- Liu, W., Chen, J., Tang, Z., Liu, H., Han, D., Li, F., 2012. Theory and Practice for Building Multi-Regional Input-Output Table for 30 Provinces in China in 2007. China Statistics Press, Beijing.

- Liu, W., Tang, Z., Chen, J., 2014. Theory and Practice for Building Multi-Regional Input-Output Table for 30 Provinces in China in 2010. China Statistics Press, Beijing.
- Liu, X., Li, X., Liu, L., He, J., Ai, B., 2008. A bottom-up approach to discover transition rules of cellular automata using ant intelligence. *Int. J. Geogr. Inf. Sci.* 22, 1247–1269.
- Liu, X., Liang, X., Li, X., Xu, X., Ou, J., Chen, Y., Li, S., Wang, S., Pei, F., 2017. A future land use simulation model (FLUS) for simulating multiple land use scenarios by coupling human and natural effects. *Landsc. Urban Plan.* 168, 94–116.
- Liu, Y., Liu, Y., Chen, Y., Long, H., 2010. The process and driving forces of rural hollowing in China under rapid urbanization. *J. Geogr. Sci.* 20, 876–888.
- Mekonnen, M.M., Hoekstra, A.Y., 2016. Four billion people facing severe water scarcity. *Sci. Adv.* 2, e1500323.
- Meng, X., Han, J., Huang, C., 2017. An improved vegetation adjusted nighttime light urban index and its application in quantifying spatiotemporal dynamics of carbon emissions in China. *Remote Sens.* 9, 829.
- Mi, Z.F., Meng, J., Guan, D.B., Shan, Y.L., Song, M.L., Wei, Y.M., Liu, Z., Hubacek, K., 2017. Chinese CO₂ emission flows have reversed since the global financial crisis. *Nat. Commun.* 8, 1712.
- Miller, R.E., Blair, P.D., 2009. Input-output Analysis: Foundations and Extensions. Cambridge university press.
- Ministry of Water Resources, N.B.o.S., 2013. Bulletin of First National Census for Water. China Water and Power Publisher, Beijing.
- O'Neill, B.C., Kriegler, E., Ebi, K.L., Kemp-Benedict, E., Riahi, K., Rothman, D.S., van Ruijven, B.J., van Vuuren, D.P., Birkmann, J., Kok, K., Levy, M., Solecki, W., 2017. The roads ahead: narratives for shared socioeconomic pathways describing world futures in the 21st century. *Glob. Environ. Chang.* 42, 169–180.
- Oki, T., Kanae, S., 2004. Virtual water trade and world water resources. *Water Sci. Technol.* 49, 203–209.
- Pontius, R.G., Boersma, W., Castella, J.C., Clarke, K., de Nijs, T., Dietzel, C., Duan, Z., Fotsing, E., Goldstein, N., Kok, K., Koomen, E., Lippitt, C.D., McConnell, W., Sood, A. M., Pijanowski, B., Pithadia, S., Sweeney, S., Trung, T.N., Veldkamp, A.T., Verburg, P.H., 2008. Comparing the input, output, and validation maps for several models of land change. *Ann. Reg. Sci.* 42, 11–37.
- Pontius, R.G., Peethambaram, S., Castella, J.-C., 2011. Comparison of three maps at multiple resolutions: a case study of land change simulation in cho don district, vietnam. *Ann. Assoc. Am. Geogr.* 101, 45–62.
- Riahi, K., van Vuuren, D.P., Kriegler, E., Edmonds, J., O'Neill, B.C., Fujimori, S., Bauer, N., Calvin, K., Dellink, R., Fricko, O., Lutz, W., Popp, A., Cuartero, J.C., Samir, K.C., Leimbach, M., Jiang, L.W., Kram, T., Rao, S., Emmerling, J., Ebi, K., Hasegawa, T., Havlik, P., Humpenoder, F., da Silva, L.A., Smith, S., Stehfest, E., Bosetti, V., Eom, J., Gernaat, D., Masui, T., Rogelj, J., Strefler, J., Drouet, L., Krey, V., Luderer, G., Harmsen, M., Takahashi, K., Baumstark, L., Doelman, J.C., Kainuma, M., Klimont, Z., Marangoni, G., Lotze-Campen, H., Obersteiner, M., Tabeau, A., Tavoni, M., 2017. The Shared Socioeconomic Pathways and their energy, land use, and greenhouse gas emissions implications: an overview. *Glob. Environ. Chang.* 42, 153–168.
- Rienow, A., Goetzke, R., 2015. Supporting SLEUTH - enhancing a cellular automaton with support vector machines for urban growth modeling. *Comput. Environ. Urban* 49, 66–81.
- Rodriguez, C.I., de Galarraga, V.A.R., Kruse, E.E., 2015. Analysis of water footprint of potato production in the pampean region of Argentina. *J. Clean. Prod.* 90, 91–96.
- Saaty, T.L., 1990. How to make a decision: the analytic hierarchy process. *Eur. J. Oper. Res.* 48, 9–26.
- Sohl, T., Sayler, K., 2008. Using the FORE-SCE model to project land-cover change in the southeastern United States. *Ecol. Model.* 219, 49–65.
- Thapa, R.B., Murayama, Y., 2011. Urban growth modeling of Kathmandu metropolitan region, Nepal. *Comput. Environ. Urban* 35, 25–34.
- Van Asselen, S., Verburg, P.H., 2013. Land cover change or land-use intensification: simulating land system change with a global-scale land change model. *Glob. Chang. Biol.* 19, 3648–3667.
- Verburg, P.H., Soepboer, W., Veldkamp, A., Limpiada, R., Espaldon, V., Mastura, S.S.A., 2002. Modeling the spatial dynamics of regional land use: the CLUE-S model. *Environ. Manag.* 30, 391–405.
- Vörösmarty, C.J., Hoekstra, A.Y., Bunn, S.E., Conway, D., Gupta, J., 2015. Fresh water goes global. *Science* 349, 478–479.
- WWAP, 2019. The United Nations World Water Development Report 2019: Leaving No One behind. United Nations Educational, Scientific and Cultural Organization (UNESCO), Paris.
- Yeh, A.G.O., Li, X., 2006. Errors and uncertainties in urban cellular automata. *Comput. Environ. Urban* 30, 10–28.
- Zhang, C., Anadon, L.D., 2014. A multi-regional input-output analysis of domestic virtual water trade and provincial water footprint in China. *Ecol. Econ.* 100, 159–172.
- Zhang, D., Huang, Q.X., He, C.Y., Wu, J.G., 2017. Impacts of urban expansion on ecosystem services in the Beijing-Tianjin-Hebei urban agglomeration, China: a scenario analysis based on the Shared Socioeconomic Pathways. *Resour. Conserv. Recycl.* 125, 115–130.
- Zhang, Y., Chen, Y., Huang, M., 2018. Water footprint and virtual water accounting for China using a multi-regional input-output model. *Water* 11, 34.
- Zhang, Z., Yang, H., Shi, M., 2011. Analyses of water footprint of Beijing in an interregional input–output framework. *Ecol. Econ.* 70, 2494–2502.